Proc. Nat. Acad. Sci. USA
Vol. 69, No. 9, pp. 2437–2441, September 1972

Structure and Properties of a Synthetic Analogue of Bacterial Iron–Sulfur Proteins

(Fe_4S_4 core/PMR-iron–sulfur complexes/x-ray diffraction)

T. HERSKOVITZ*, B. A. AVERILL*, R. H. HOLM*†, JAMES A. IBERS‡,
W. D. PHILLIPS§, AND J. F. WEIHER§

* Department of Chemistry, Massachusetts Institute of Technology, Cambridge, Mass. 02139; ‡Department of Chemistry, Northwestern University, Evanston, Illinois 60201; and §Central Research Department, E. I. du Pont de Nemours and Company, Wilmington, Delaware 19898

Contributed by W. D. Phillips, June 21, 1972

ABSTRACT **The compound $(Et_4N)_2[Fe_4S_4(SCH_2Ph)_4]$ has been prepared and its structure determined by x-ray diffraction. The Fe_4S_4 core of the anion possesses a configuration of D_{2d} symmetry that is closely related to the Fe_4S_4 active-site structures of the high-potential iron protein from *Chromatium* and the ferredoxin from *Micrococcus aerogenes*. Electronic properties of the tetrameric anion have been partially characterized by measurement of proton magnetic resonance, Mössbauer, photoelectron, and electronic spectra, and magnetic susceptibility. Comparison of corresponding properties of $[Fe_4S_4(SCH_2Ph)_4]^{2-}$ and the proteins implies that the oxidation levels of the synthetic tetramer, the reduced form of the high-potential protein, and the oxidized form of the 8-Fe ferredoxins are equivalent. The tetramer possesses the one-electron redox capacity associated with the 4-Fe centers of the ferredoxins. The structural and collective electronic features of $[Fe_4S_4(SCH_2Ph)_4]^{2-}$ reveal it to be the first well-defined synthetic analogue of the active site of an iron–sulfur protein.**

Nonheme iron–sulfur proteins are active in electron transport processes in the metabolism of bacteria, plants, and mammals (1). The ubiquitous occurrence of these proteins in various organisms, together with their unusual and characteristic electronic features (2), has stimulated intense research activity that has resulted in the isolation of several of proteins of low molecular weight (about 6,000–30,000), and the accumulation of extensive data on their physical properties. Iron and sulfur are involved in the active sites of many of these proteins, but a full structural and electronic characterization of these sites in proteins containing more than one iron atom has not been achieved. Furthermore, the postulated or known structures and the measured electronic properties of the active sites of such proteins have not been duplicated or closely approached in any synthetic species of well-defined stoichiometry and structure. Recent x-ray studies have specified the overall structures of the iron–sulfur active sites of three types of bacterial proteins, containing one, four, and eight iron atoms and zero, four, and eight atoms of acid-labile or "inorganic" sulfur (S*), respectively. Rubredoxin from *Clostridium pasteurianum* contains a distorted tetrahedral Fe-S_4 unit (3, 4). The high-potential iron protein from *Chromatium* (2.25-Å resolution) possesses a roughly cubic Fe_4S_4* cluster, with iron and sulfur atoms at alternate vertices (5). Recent results on the 8Fe-8S* clostridial ferredoxin from *M. aerogenes* indicate the presence of two Fe_4S_4* clusters, separated by 12 Å, each of which has a structure similar to that of the cluster in high-potential iron protein (6). Each iron of the cluster is bound to the polypeptide chain by one mercaptide sulfur from a cysteinyl residue. The occurrence of a structurally related Fe_4S_4 unit in synthetic compounds has been established only for $[(h^5\text{-}C_5H_5)FeS]_4$ (7, 8), but may also exist in the tetrameric dithiolene complexes $[Fe_4S_4(S_2C_2R_2)_4]^z$ (9). Other recent studies of synthetic iron–sulfur complexes have centered principally on two-iron species containing mercaptide (10) and sulfide (2, 11, 12) bridges. Certain of the latter evidence spectral similarities to the plant ferredoxins, for which the $(Cys\text{-}S)_2Fe\text{-}S_2$*–$Fe(S\text{-}Cys)_2$ arrangement is most probable (2, 13), but none of these complexes has been definitely characterized in solution or in the solid state.

We report results clearly demonstrating that a structure closely related to that of the active site of four- and eight-iron bacterial proteins can be stabilized in discrete synthetic complexes lacking a cysteinyl-containing polypeptide component. These complexes are of the general formulation $[Fe_4S_4(SR)_4]^{2-}$ (R = alkyl), in which each iron atom is bonded to three bridging sulfurs and one terminal mercaptide. As the results described below indicate, certain of the electronic properties of these species resemble those of the proteins in given oxidation levels. Hence, their structural and electronic features reveal these complexes to be the first synthetic analogues of the active sites of iron–sulfur proteins.

MATERIALS AND METHODS

The complexes $[Fe_4S_4(SR)_4]^{2-}$ were prepared by reaction of ferric chloride, sodium methoxide, sodium hydrosulfide, and the appropriate alkyl mercaptan in methanol solution, and were isolated as their tetraalkylammonium salts. They were purified by repeated recrystallization from acetonitrile. Full synthetic details will be presented elsewhere (T. Herskovitz, B. A. Averill, R. H. Holm, and J. A. Ibers, to be published). The R = benzyl species is typical of complexes of this type; it has been thoroughly characterized as its tetraethylammonium salt. *Anal.* Calcd. for $C_{44}H_{68}N_2S_8Fe_4$: C, 47.83; H, 6.20; N, 2.54; S, 23.21; Fe, 20.22. Found: C, 47.72; H, 6.35; N, 2.59; S, 23.14; Fe, 20.25; mp 123–124°C (evacuated tube). The analogous R = CH_3 compound was obtained in an equivalent state of purity. These compounds are soluble in polar organic solvents and are stable in solution and in the solid phase in the absence of oxygen.

† To whom correspondence should be addressed.

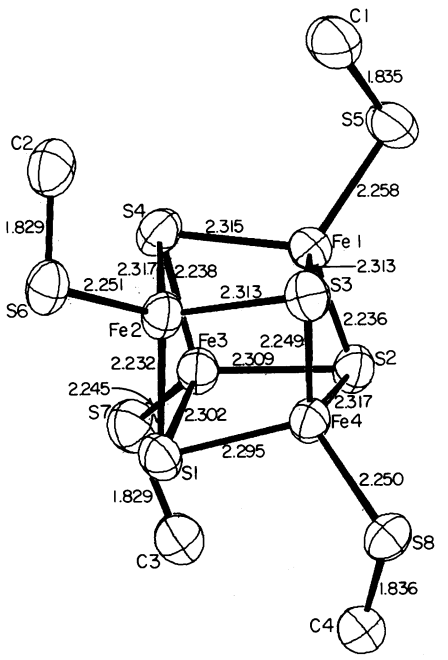

FIG. 1. The inner portion of the $[Fe_4S_4(SCH_2Ph)_4]^{2-}$ anion; 50% probability ellipsoids of thermal vibration are shown; hydrogen atoms are omitted for the sake of clarity.

X-Ray Data and Structural Solution. $(Et_4N)_2[Fe_4S_4(SCH_2Ph)_4]$ was obtained as well-formed red-black crystals stable to x-rays. The crystals belong to the monoclinic system, space group C_{2h}^5-$P2_1/c$ (uniquely determined). Cell dimensions are $a = 11.922(6), b = 34.523(17), c = 12.762(5)$ Å, $\beta = 95.78(2)°$ (based on $\lambda(MoK_{\alpha 1}) = 0.70930$ Å, $t = 23°$). $d_{obs} = 1.43(3)$ g/cm³ by flotation in aqueous zinc chloride solution; $d_{calc} = 1.40$ g/cm³ for $Z = 4$. Linear absorption coefficient (Mo radiation) = 13.6 cm^{-1}. Data were collected on a Picker FACS-1 automatic diffractometer, using MoK_α radiation monochromatized from the (002) face of a highly mosaic graphite crystal. The crystal used in the data collection had approximate dimensions of 1.0 mm × 0.2 mm × 0.5 mm (calculated volume = 0.814 mm³). A total of 5047 independent reflections was collected. Of these, 4089 obeyed the condition $I > 3\sigma(I)$, where $\sigma(I)$ is based on the total counting statistics and a $P = 0.03$ (14). Data were processed (14), and only the 4084 reflections above 3σ were carried in the ensuing calculations. The structure was solved by direct methods, with the aid of the programs FAME (Dewar) for obtaining normalized structure factors, and the MULTAN series (Main, Woolfson, and Germain). The best solution, based on 408 normalized structure factors, yielded the correct positions for the four Fe and eight S atoms. The other nonhydrogen atoms were found in a subsequent difference Fourier synthesis. The structure was refined by full-matrix least-squares methods until anisotropic thermal parameters were added, at which time division of the matrix into two blocks was necessary. The quantity minimized was $\Sigma\omega(|F_o|-|F_c|)^2$, where $|F_o|$ and $|F_c|$ are the observed and calculated structure amplitudes and the weights, ω, were taken as $4F_o^2/\sigma^2(F_o^2)$. Refinement of a completely isotropic model, with no hydrogen atoms, converged to a conventional R factor of 11%. Because of the excessive number of parameters, anisotropic refinement was done with two blocks of the least-squares matrix. All nonhydrogen atoms were refined anisotropically, except for the carbon atoms in the rigid phenyl groups that were assigned variable individual isotropic thermal parameters. After convergence was achieved, the contributions of the hydrogen atoms were added. A difference Fourier synthesis revealed the positions of all methyl hydrogens. For the methylene hydrogens, positions were calculated on the assumption of d(C–H) = 1.0 Å and tetrahedral geometry, and these atoms were assigned the equivalent isotropic thermal parameters of the carbon atoms to which they are attached. Refinement was continued until convergence, at which point R = 3.6%.

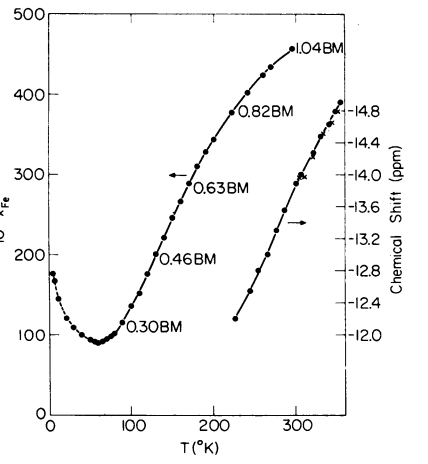

FIG. 2. Temperature dependences of the paramagnetic component of the magnetic susceptibility per iron atom and methylene proton chemical shifts (●, acetonitrile, ×, dimethylsulfoxide solution) of $(Et_4N)_2[Fe_4S_4(SCH_2Ph)_4]$. Magnetic moments per iron, as calculated from the Curie law, are given at selected temperatures. Pascal's constants were used to correct for molecular diamagnetism.

TABLE 1. *Average values of principal distances and angles in the Fe_4S_8 core of $(Et_4N)_2[Fe_4S_4(SCH_2Ph)_4]$*

Type	Number	Distance (Å) or angle (deg)*	Remarks
Fe(1)–S(3)	8	2.310(3)	Fe–sulfide
Fe(1)–S(2)	4	2.239(4)	Fe–sulfide
Fe(1)–S(5)	4	2.251(3)	Fe–mercaptide
Fe(1)–Fe(2)	2	2.776(10)	
Fe–Fe (other)	4	2.732(5)	
S(1)–S(2)	2	3.645(3)	sulfide–sulfide
S–S (other)	4	3.586(7)	sulfide–sulfide
Fe–Fe–Fe	4	61.1(3)	
Fe–Fe–Fe	8	59.5(2)	
S–S–S	4	61.1(1)	sulfide
S–S–S	8	59.4(2)	sulfide
S–Fe–S	12	104.1(2)	sulfide
Fe–S–Fe	12	73.8(3)	sulfide
S–Fe–S	12	111.7–117.3	sulfide–Fe–mercaptide

* The numbers in parentheses are standard deviations, estimated from the agreement among the averaged distances or angles.

Proton magnetic resonance measurements were made on Varian HA-100 and HR-220 spectrometers, and are internally referenced to tetramethylsilane. Mössbauer spectra were obtained with a Nuclear Science Instruments spectrometer.

Spectra were fit with a least-squares computer program; Lorentzian line shapes were assumed. Magnetic susceptibilities were determined by the Faraday method with $HgCo(NCS)_4$ as the calibrant. Electrochemical measurements were made as described (15); half-wave potentials are given at 25°C against a saturated calomel electrode.

RESULTS AND DISCUSSION

Description of the structure

The crystal structure of $(Et_4N)_2[Fe_4S_4(SCH_2Ph)_4]$ consists of well-separated cations and anions. The cations have their expected geometry (with no evidence of disorder), and will not be considered further. The Fe_4S_4 core of the anion is a distorted cube, with iron and sulfur atoms at alternate vertices. The principal dimensions of the core, together with the atom labeling system, are given in Fig. 1. Listed in Table 1 are the average distances and angles for the Fe_4S_8 portion of the anion.

As is seen in Fig. 1 and from the data in Table 1, the Fe_4S_4 core exhibits obvious distortions from cubic symmetry. In particular, the angles S–Fe–S are 104.1°, while the angles Fe–S–Fe are 73.8°, so that each face of the polyhedron is a rhomb. These rhombs are distinctly nonplanar. There are six planes through the Fe_4S_4 portion of the anion that are perfect within experimental error. These are the diagonal planes defined by the atoms Fe(n), Fe(m), S(n), S(m), where $1 \leqslant n \leqslant 3$ and $n < m \leqslant 4$. The distortions of this portion of the complex from cubic symmetry are essentially those of the point group $D_{2d}-\bar{4}2m$, where the $\bar{4}$ axis passes through the top and bottom faces of the polyhedron in Fig. 1. There is a slight compression of the polyhedron along this axis. The significant variation in the sulfide–Fe–mercaptide bond angles probably result from packing effects, since the mercaptide sulfurs are attached to the bulky benzyl groups, and the packing of the crystal structure is primarily between these groups and the cations.

A further significant feature of the $[Fe_4S_4(SCH_2Ph)_4]^{2-}$ structure is the apparent lack of distinction between iron atoms. If the core sulfur is considered as S^{2-} the complex formally contains one pair each of Fe(II) and Fe(III). Structural parameters of each iron site are insignificantly different, and it can only be noted that the Fe–S(mercaptide) distance is closed to those values found in complexes where the metal may be unambiguously regarded as Fe(III). Corresponding distances in $[Fe(S_2CEt)_2(SEt)]_2$ and $[Fe(SCH_2CH_2S)_2]_2^{2-}$ are 2.22 Å (16) and 2.22–2.26 Å (M. R. Snow, J. A. Ibers, T. Herskovitz, and R. H. Holm, to be published), respectively. No distinction can be made between static disorder and a symmetrically delocalized (D_{2d}) structure.

The closest structural analogue (of synthetic origin) to $[Fe_4S_4(SCH_2Ph)_4]^{2-}$ is $[(h^5\text{-}C_5H_5)FeS]_4$ (7, 8). This species also contains a Fe_4S_4 core of D_{2d} symmetry, with a pentahaptocyclopentadienyl group bonded to each iron. There are important structural differences between the two species. In a qualitative sense the iron atoms are toward the outside of the polyhedron in the neutral molecule, while in the anion they are toward the inside. Whereas the anion contains essentially equivalent Fe–Fe distances of about 2.75 Å, each iron in the neutral species[¶] has one Fe neighbor at 2.65 Å and two nonbonded Fe neighbors at 3.37 Å. Moreover, in the anion, all S···S distances are around 3.61 Å, while in the neutral species these distances divide into sets of 3.33 Å and 2.88 Å, corresponding to S(3)–S(4) and S(3)–S(1, 2), respectively, in Fig. 1. As a result of the differences in bond lengths, the neutral molecule has S–Fe–S independent angles of 98.2° (two) and 80.6° (four), while the Fe–S–Fe angles are two at 73.0° and four at 98.0°. The corresponding S–Fe–S and Fe–S–Fe angles in the anion are 104.1° and 73.8°.

Recently, Carter *et al.* (5) have described the active-site structure of *Chromatium* high-potential iron protein at 2.25 Å resolution. They have reached the following important conclusions: (*i*) the mean Fe–Fe distance is 3.06 Å (estimated precision ±0.14 Å), and there is good evidence that the Fe–Fe distances are equivalent; (*ii*) the Fe–S* (sulfide) distances average to 2.35 Å (precision ±0.24 A); (*iii*) the Fe–S(Cys) distances average to 2.01 Å (precision ±0.26 Å); (*iv*) the Fe_4S_4 cluster has D_{2d} symmetry, within the errors of the determination; (*v*) it is unlikely that the Fe–Fe distances resemble in detail those in $[(h^5\text{-}C_5H_5)FeS]_4$. Carter *et al.* conclude that "the high-potential iron protein cluster closely resembles a portion of the inorganic compound $(C_5H_5FeS)_4$, but the differences between the two may eventually prove more interesting than their similarities." From the data presented here it is clear that, at the present stage of refinement of the protein structure, there are significant similarities between the structures of the Fe_4S_8 units in high-potential iron protein and in $[Fe_4S_4(SCH_2Ph)_4]^{2-}$, as well as between the Fe_4S_4 units in this protein and in $[(h^5\text{-}C_5H_5)FeS]_4$. However, the suitability of the latter as an active-site analogue is diminished by the distinctly nonphysiological nature and specific electronic features of the terminal cyclopentadienyl ligands. The similarity of the organic mercaptide groups in $[Fe_4S_4(SR)_4]^{2-}$ to cysteinyl residues in the proteins is apparent. The precise relationship of the structure of high-potential iron protein or of the synthetic tetramers to that of ferredoxin from *M. aerogenes* (6) cannot be assessed until the structure of the ferredoxin is reported in more detail.

In addition to structural similarities, $[Fe_4S_4(SCH_2Ph)_4]^{2-}$ and the active sites of *Chromatium* high-potential iron protein and the bacterial ferredoxins appear to bear striking electronic resemblances. Each of the latter exists in two oxidation levels differing by one electron per 4-Fe center, and magnetic properties (2) are consistent with a spin-singlet (S = 0) ground state for each such center in ferredoxin$_{(ox)}$ and in high-potential iron protein$_{(red)}$. The following results suggest a relationship between even-electron $[Fe_4S_4(SCH_2Ph)_4]^{2-}$ and these forms of the proteins. Oxidized ferredoxins from *Cl. pasteurianum* (17) and *Cl. acidi-urici* (18) display in solution magnetic moments per iron (μ_{Fe}) less than the lower limit of 1.73 Bohr magnetons for magnetically dilute spin-paired Fe(III), and a positive temperature coefficient of μ_{Fe}. The isotropic contact shifts of PMR signals tentatively associated by Poe *et al.* (17, 18) with the β-CH_2 groups of cysteinyl residues of these proteins also increase with increasing temperature. Contact-shifted resonances of high-potential iron protein$_{(red)}$ behave similarly (19); this form of the protein is essentially diamagnetic by bulk-susceptibility measurements (20). These results, all but the last of which were obtained over a limited temperature range (about 5–50°C) in solution, have been interpreted in terms of antiferromagnetic exchange coupling between the metal centers. Solid-state magnetic susceptibility results and methylene proton chemical shifts for $[Fe_4S_4(SCH_2Ph)_4]^{2-}$, obtained over much-wider temperature intervals, are presented in Fig.

[¶] The structural data quoted refer to the monoclinic form (8). Corresponding data for the orthorhombic phase are closely similar (7).

TABLE 2. *Mössbauer results for* $(Et_4N)_2[Fe_4S_4(SCH_2Ph)_4]$

Quantity (mm/sec)	296°K	78°K	4.2°K
Isomer shift*	+0.60	+0.58	+0.58
Isomer shift†	+0.33	+0.32	+0.32
ΔE_Q	1.10	1.26	1.25
Γ‡	0.6 ± 0.2	0.31 ± 0.02	0.33 ± 0.02

* ^{57}Fe isomer shift *versus* that of sodium nitroprusside.
† ^{57}Fe isomer shift *versus* that of iron metal.
‡ Linewidth at half-maximum.

2. Paramagnetic susceptibilities and magnetic moments per iron are given. The increase in χ_{Fe} (or μ_{Fe}) and PMR contact shifts with temperature are clearly indicative of an antiferromagnetically coupled Fe_4 unit. The rise in susceptibility below about 60°K is attributed to the presence of a very small amount of high-spin Fe(III) impurity. The μ_{Fe} value of 1.04 Bohr magnetons (296°K) accords well with ambient temperature values of 1.1–1.2 Bohr magnetons for *Cl. pasteurianum* ferredoxin (17, 21) and 1.2 Bohr magnetons for *Cl. acidi-urici* ferredoxin (18). A single methylene proton resonance is observed for $[Fe_4S_4(SCH_2Ph)_4]^{2-}$ in dimethylsulfoxide or acetonitrile solution and, as is the case for signals assigned to β-CH_2 groups that are in a corresponding structural position in the 4-Fe and 8-Fe proteins, this resonance experiences a progressively negative isotropic shift as the temperature is increased.

The ^{57}Fe Mössbauer spectrum of $(Et_4N)_2[Fe_4S_4(SCH_2Ph)_4]$ consists of a single quadrupole-split doublet. Results are summarized in Table 2. Mössbauer results for relevant bacterial proteins are currently limited, with data having been reported for the oxidized and reduced forms of *Chromatium* high-potential iron protein (22, 23), *Chromatium* ferredoxin (22), and *Cl. pasteurianum* ferredoxin (24). The following parameters (isomer shift against Fe, ΔE_Q) obtained at 77°K may be compared with those in Table 2: high-potential iron protein$_{(red)}$, +0.42, 1.12 mm/sec (23); ferredoxin$_{(ox)}$, about +0.26, 0.93 mm/sec (24). This comparison also suggests an electronic similarity between $[Fe_4S_4(SCH_2Ph)_4]^{2-}$ and the protein active sites. Unlike ferredoxin$_{(ox)}$ from *Cl. pasteurianum* (24), the spectrum of $[Fe_4S_4(SCH_2Ph)_4]^{2-}$ presents no indication of two overlapping doublets with very similar isomer shifts and quadrupole coupling constants.

Photoelectron spectra of $(Et_4N)_2[Fe_4S_4(SCH_2Ph)_4]$ have been determined, and the following binding energies and linewidths at half-maximum intensity obtained: Fe(3*s*), 102.4 ± 0.1 ,2.4 eV; S (2*p*), 161.8 ± 0.1, 2.7 eV. Binding energies were measured relative to C(1*s*) at 285.0 eV. The S(2*p*) binding energies fall in the narrow interval (161.5–163.2 eV) recently found for high-potential iron protein$_{(red)}$ and ferredoxin$_{(ox)}$ (25). Unlike the results for the proteins, where computer analysis of the spectra indicates an about 1.5 eV difference in binding energy between mercaptide and sulfide sulfur, no evidence of observably different binding energies for the two types of sulfur was found. The Fe(3*s*) spectrum consisted of a single symmetrical line, with no evidence of inequivalent iron sites.

Finally, the electronic spectrum and redox properties of $[Fe_4S_4(SCH_2Ph)_4]^{2-}$ in acetonitrile solution have been investigated. A characteristic feature of the spectra of 4-Fe and 8-Fe proteins is the presence of a prominent absorption band in the 380–400 nm region that is definitely associated with the iron–sulfur chromophore (2). In high-potential iron protein$_{(red)}$ this band occurs at 388 nm (ϵ 16,100) (26), and in ferredoxin$_{(ox)}$—such as that from *Cl. acidi-urici*—it is found at 390 nm (ϵ 30,600) (27). An apparently related feature is observed in the spectrum of the synthetic tetramer, whose intensity at 417 nm (ϵ 19,400) is comparable with those of the 4-Fe units of the proteins. In addition, the spectrum of the tetramer contains a shoulder at 290 nm (ϵ 31,000), close to where other absorption bands of high-potential iron protein$_{(red)}$ and ferredoxin$_{(ox)}$ are found (26, 27). Electrochemical measurements confirm that the tetramer further resembles the 8-Fe proteins in redox properties. In view of the structure of *M. aerogenes* ferredoxin (6), the two-electron acceptor properties of various ferredoxin$_{(ox)}$ (2) may now be interpreted in terms of one-electron reduction of each Fe_4S_4* cluster. Polarographic and cyclic voltammetric studies reveal that the tetramer undergoes the reversible one-electron transfer process, $[Fe_4S_4(SCH_2Ph)_4]^{3-} \rightleftharpoons [Fe_4S_4(SCH_2Ph)_4]^{2-} + e^-$, $E_{1/2} = -1.19$ V. This half-wave potential is more cathodic than that found for ferredoxin$_{(red)} \rightleftharpoons$ ferredoxin$_{(ox)} + e^-$ [−0.57 V against saturated calomel electrode (pH 7)] obtained from measurement of *Cl. pasteurianum* ferredoxin (28); the difference may be due in part to medium effects and, as with other comparisons of electronic properties, to as yet undetermined structural variations. No other reduction process was observed in cathodic scans to −1.7 V. $[Fe_4S_4(SCH_2Ph)_4]^{2-}$ also undergoes an irreversible oxidation at about −0.15 V with a dropping-mercury electrode. The oxidation has not been satisfactorily characterized at a platinum electrode, due to absorption of the oxidized product on the electrode. Aerial oxidation results in decomposition of the tetramer. Further investigation is required to establish any relationship between the electrochemical oxidation of the tetramer and the process high-potential iron protein$_{(red)} \rightleftharpoons$ high-potential iron protein$_{(ox)} + e^-$, for which E_m (pH 7) = +0.35 V (26).

We draw the following principal conclusions from our present results: (*i*) stable tetrameric units of the type $[Fe_4S_4(SR)_4]^{2-}$ can be formed in the absence of a cysteinyl-containing polypeptide; (*ii*) the structure of $[Fe_4S_4(SCH_2Ph)_4]^{2-}$ is clearly similar to the active site of *Chromatium* high-potential iron protein and, presumably, to the active sites of 8-Fe proteins; (*iii*) comparative electronic properties (particularly magnetic susceptibilities, Mössbauer parameters, and electronic spectra) imply that $[Fe_4S_4(SCH_2Ph)_4]^{2-}$ and the active sites of ferredoxin$_{(ox)}$ and high-potential iron protein$_{(red)}$ possess equivalent levels of oxidation; (*iv*) $[Fe_4S_4(SCH_2Ph)_4]^{2-}$ exhibits a redox capacity consistent with that for the Fe_4S_4* clusters of 8-Fe proteins; (*v*) measurements capable of detecting widely different lifetimes of structural and electronic configurations (about 10^{-3} sec (PMR) to about 10^{-16} sec (photoelectron spectroscopy, x-ray diffraction)) suggest that a fully delocalized electronic description of the Fe_4S_4 core of $[Fe_4S_4(SCH_2Ph)_4]^{2-}$ is more meaningful than a designation in terms of the formal oxidation states 2 Fe(II), 2 Fe(III), and $4S^{2-}$. Work currently in progress is directed toward the synthesis of additional $Fe_4S_4(SR)_4$ tetramers and a further elucidation of their structural and electronic properties in accessible levels of oxidation.

We are indebted to Dr. J. E. Lester for measurement of photoelectron spectra. This research was supported at M.I.T. by

Research Grants GP-18978X (National Science Foundation) and GM-19256 (National Institutes of Health), and at Northwestern University by Research Grant HE-13157 (National Institutes of Health). This is contribution No. 1954 from the Central Research Department of DuPont.

1. Buchanan, B. B. & Arnon, D. I. (1970) *Advan. Enzymol.* **33,** 119–176.
2. Tsibris, J. C. M. & Woody, R. W. (1970) *Coord. Chem. Rev.* **5,** 417–458.
3. Herriott, J. R., Sieker, L. C., Jensen, L. H. & Lovenberg, W. (1970) *J. Mol. Biol.* **50,** 391–406.
4. Watenpaugh. K. D., Sieker, L. C., Herriott, J. R. & Jensen, L. H. (1971) *Cold Spring Harbor Symp. Quant. Biol.* **36,** 359–367.
5. Carter, C. W., Jr., Freer, S. T., Xuong, Ng. H., Alden, R. A., & Kraut, J. (1971) *Cold Spring Harbor Symp. Quant. Biol.* **36,** 381–385.
6. Sieker, L. C., Adman, E. & Jensen, L. H. (1972) *Nature* **235,** 40–42.
7. Schunn, R. A., Fritchie, C. J., Jr. & Prewitt, C. T. (1966) *Inorg. Chem.* **5,** 892–899.
8. Wei, C. H., Wilkes, G. R., Treichel, P. M. & Dahl, L. F., (1966) *Inorg. Chem.* **5,** 900–905.
9. Balch, A. L. (1969) *J. Amer. Chem. Soc.* **91,** 6962–6967.
10. Coucouvanis, D., Lippard, S. J. & Zubieta, J. A. (1970) *J. Amer. Chem. Soc.* **92,** 3342–3347; Clare, M., Hill, H. A. O., Johnson, C. E. & Richards, R. (1970) *Chem. Commun.* 1376–1377; Connelly, N. G. & Dahl, L. F. (1970) *J. Amer. Chem. Soc.* **92,** 7472–7474.
11. Yang, C. S. & Huennekens, F. M. (1970) *Biochemistry* **9,** 2127–2133.
12. Sugiura, Y. & Tanaka, H. (1972) *Biochem. Biophys. Res. Commun.* **46,** 335–340.
13. Dunham, W. R., Palmer, G., Sands, R. H. & Bearden, A. J. (1971) *Biochim. Biophys. Acta* **253,** 373–384.
14. Corfield, P. W. R., Doedens, R. J. & Ibers, J. A. (1967) *Inorg. Chem.* **6,** 197–204.
15. Forbes, C. E., Gold, A., & Holm, R. H. (1971) *Inorg. Chem.* **10,** 2479–2485.
16. Coucouvanis, D., Lippard, S. J. & Zubieta, J. A. (1970) *Inorg. Chem.* **9,** 2775–2781.
17. Poe, M., Phillips, W. D., McDonald, C. C. & Lovenberg, W. (1970) *Proc. Nat. Acad. Sci. USA* **65,** 797–804.
18. Poe, M., Phillips, W. D., McDonald, C. C. & Orme-Johnson, W. H. (1971) *Biochem. Biophys. Res. Commun.* **42,** 705–713.
19. Phillips, W. D., Poe, M., McDonald, C. C. & Bartsch, R. D. (1970) *Proc. Nat. Acad. Sci. USA* **67,** 682–687.
20. Moss, T. H., Petering, D. & Palmer, G. (1969) *J. Biol. Chem.* **244,** 2275–2277.
21. Druskeit, W., Gersonde, K. & Netter, H. (1967) *Eur. J. Biochem.* **2,** 176–181.
22. Moss, T. H., Bearden, A. J., Bartsch, R. G., Cusanovich, M. A. & San Pietro, A. (1968) *Biochemistry* **7,** 1591–1596.
23. Evans, M. C. W., Hall, D. O. & Johnson, C. E. (1970) *Biochem. J.* **119,** 289–291.
24. Blomstrom, D. C., Knight, E., Jr., Phillips, W. D. & Weiher, J. F. (1964) *Proc. Nat. Acad. Sci. USA* **51,** 1085–1092.
25. Kramer, L. N. & Klein, M. P. (1972) in *Electron Spectroscopy,* ed. Shirley, D. A. (North-Holland Publishing Co., Amsterdam), pp. 733–751.
26. Dus, K., DeKlerk, H., Sletten, K. & Bartsch, R. G. (1967) *Biochim. Biophys. Acta* **140,** 291–311.
27. Hong, J. S. & Rabinowitz, J. C. (1970) *J. Biol. Chem.* **245,** 4982–4987.
28. Weitzman, P. D. J., Kennedy, I. R. & Caldwell, R. A. (1971) *FEBS Lett.* **17,** 241–244.